Prediction of the Madden-Julian Oscillation and its impact on the European weather in the ECMWF monthly forecasts

Frédéric Vitart, Franco Molteni and Thomas Jung

ECMWF, Shinfield Park, Reading
RG2 9AX, United Kingdom
nec@ecmwf.int

ABSTRACT

A series of 46-day ensemble integrations starting on the 15^{th} of each month from 1989 to 2008 has been completed with the European Centre for Medium-Range Weather Forecasts (ECMWF) forecast system. The Madden Julian Oscillation (MJO) simulated by the hindcasts is diagnosed using an index based on combined empirical orthogonal functions (EOFs) of zonal winds at 200 and 850 hPa and Outgoing Longwave radiation (OLR). Results indicate that the dynamical model is able to maintain the amplitude of the MJO during the 46 days of integrations and the model displays skill for up to about twenty days to predict the evolution of the MJO. However, the MJO simulated by the model has a too slow eastward propagation and has difficulties crossing the Maritime Continent.

The MJO teleconnections simulated by the ECMWF forecast system have been compared to reanalysis. In the Northern Extratropics, the MJO simulated by the model has an impact on North Atlantic weather regimes, most particularly on the NAO, but with a smaller amplitude than in reanalysis which can be partly explained by the too slow eastward propagation of the simulated MJO events. The amplitude of the impact of the MJO over Europe also displays a large spread in the model ensemble distribution suggesting that 20-year of reanalysis may be too short to evaluate the amplitude of the impact of the MJO over Europe.

The impact of the MJO on the monthly forecast probabilistic skill scores has been assessed. Results indicate that the MJO simulated by the model has a statistically significant impact on weekly mean probabilistic skill scores in the Northern Extratropics for day 12-18, day 19-25 and 26-32. At the time range day 19-25, the reliability of the probabilistic forecasts over Europe depends strongly on the presence of an MJO event in the initial conditions. This result confirms that the MJO is a major source of predictability in the Extratropics in the sub-seasonal time scale.

The last part of this study investigates the impact of the northern extratropical circulation on the MJO skill scores. Using a series of relaxation hindcast experiments, this paper shows that the northern Extratropics have a significant impact on the skill of the ECMWF forecast system in predicting the MJO during boreal winter. Additional experiments in which the relaxation is confined to different areas of the Northern Hemisphere Extratropics suggest that it is atmospheric circulation anomalies in the western North Pacific region which most strongly affect the MJO.

1 Introduction

The Madden-Julian Oscillation (MJO) (Madden and Julian 1971) is a tropical large-scale oscillation dominated by periods of 30-60 days and zonal wavenumber-1 propagating eastward. It is the main source of potential predictability in the Tropics on time scales exceeding one week but less than a season. The maximum convective activity associated with the MJO occurs over the warm waters of the Indian Ocean and western Pacific where the MJO moves eastward at a relatively low speed (5 m s^{-1}), whereas in the western Hemisphere the MJO is less well coupled to convection and propagates faster (15 m s^{-1}). The MJO is not a regular oscillation. Instead it is episodic and its speed of propagation and duration vary from case to case. The MJO displays a strong seasonality, with more MJO events in winter

and spring, and a strong interannual variability. This makes the prediction of the MJO a challenging task for numerical weather prediction (NWP) models.

The MJO has a large impact on the Indian (e.g. Murakami 1976) and Australian monsoon (e.g. Hendon and Liebmann 1990). It plays an active role in the onset and development of an El-Niño event (e.g. Kessler and McPhaden 1995) and has an impact on tropical cyclogenesis (e.g. Nakazawa 1988). Matthews (2004) found that MJO events can be used to predict summer rainfall episodes over west Africa. The MJO also impacts the extratropical weather (e.g. Knutson and Weickmann 1987, Ferranti et al 1990, Matthews et al 2004, Donald et al 2006, Cassou 2008, Lin et al 2009). Several studies (e.g. Ferranti et al 1990; Matthews et al 2004; Cassou 2008, Lin et al. 2009) suggest that the impact of the MJO on the northern Extratropical weather is due to Rossby wave propagation. The Rossby wave propagation depends on the longitude where the convection associated to an MJO event takes place. For instance, Lin et al (2010) imposed a heat source consistent with an MJO over the Maritime continent in a linearised global primitive equation model. In this experiment, no significant impact was found in the northern Extratropics. However, when they impose a heat source over the Indian ocean or West Pacific, a Rossby wave is generated in the northern Extratropics with a pattern consistent with the observed MJO teleconnections.

Since the MJO has a significant impact on the northern Hemisphere weather, it is important for a monthly forecasting system to have skill not only in predicting the evolution of the MJO, but also in simulating the MJO teleconnections. The goal of the present paper is to evaluate the skill of a large set of 46-day hindcasts using a version of the ECMWF Integrated Forecast System (IFS) known as Cycle 32r3 (Cy32r3) (Bechtold et al. 2008) to simulate MJO events and its teleconnections in the Tropics and in the Northern Extratropics.

A first goal of this paper it to assess the skill of the numerical model to predict MJO events. The skill of the ECMWF model has so far been assessed routinely for each new model cycle using a series of 5-member ensemble integrations of 32-day forecasts for each day from 15 December 1992 till 31 January 1993 (46 cases), during the Intensive Observing Period of the Tropical Ocean Global Atmosphere Coupled Ocean-Atmosphere Response Experiment (TOGA COARE). This experimental setup has the advantage of being cheap enough to be performed for each new version of the model, and give a good indication of the MJO representation in each new version of the ECMWF model (see example in Bechtold et al. 2008). However the serial experiments cover only one single MJO event. The skill of the model to predict this specific MJO event may not be representative of the general skill of the model. In the present study, a large number of model hindcasts covering a 20 year period (1989-2008) is used to assess the skill of the ECMWF monthly forecasts. This should give a more reliable evaluation of the skill of the model than the serial experiments.

A second goal of this paper is to evaluate the impact of the MJO on the Northern Extratropics, most especially on the North Atlantic weather regimes and on the monthly forecast probabilistic skill scores. Such study would have been difficult before Cy32r3, since the model could not maintain the amplitude of an MJO event for more than a few days. Over the recent years, the representation of the MJO has improved dramatically (Fig. 1), thanks mostly to changes in the model's physics introduced in Cy32r3 (Bechtold et al. 2008). Now IFS is able to maintain the amplitude of the MJO for more than 30 days, which makes it possible to evaluate the teleconnections associated to the MJO in the model integrations.

After this introduction, Section 2 will describe the experimental setup. The skill of the model to predict MJO events will be evaluated in Section 3. Section 4 will how the impact of the MJO on the North Atlantic weather regimes in the model simulations. The impact of the MJO on monthly forecast probabilistic skill scores will be evaluated in Section 5. Section 6 will discuss the impact of the northern extratropical circulation on the MJO forecast skill scores. Finally, Section 7 will summarise the main results of this paper.

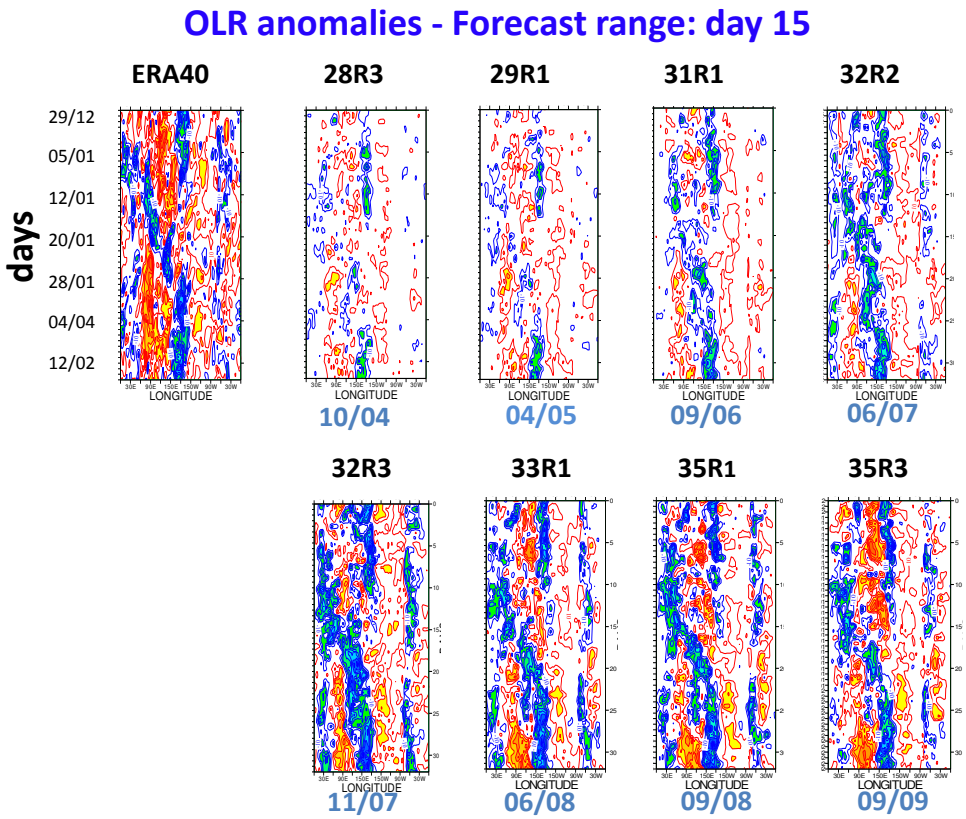

Figure 1: Series of 5-member ensemble of 32-day integrations have been performed for each day from 15 December 1992 till 31 January 1993 with the recent versions of IFS. This plot shows the Hovmoeller diagram of the ensemble mean of OLR anomalies computed from each ensemble forecast at day 15 for different versions of IFS. The top left panel shows the verification from ERA Interim. The other panels show the Hovmoeller diagrams for the version of IFS indicated above the panel and which date of operational implementation is indicated below. This plots shows that the operational prediction of the MJO has clearly improved since Cycle 32r3.

2 Experimental setup

A series of hindcasts has been performed for the 20-year period 1989 to 2008. The hindcasts start on the 15th of each month and are 46 days long in order to cover the full next calendar month. For each starting date, the hindcasts consist of an ensemble of 15 members: a control and 14 perturbed forecasts. The version of IFS used in this experiment is Cy32r3, which was operational from November 2007 until June 2008. As mentioned in the introduction, this version of IFS showed a clear improvement in the representation of the MJO compared to the previous versions. The configuration of the hindcast is the same as the one used in the operational monthly forecast at ECMWF (Vitart et al. 2008) except for the length of the forecasts (46 days instead of 32 days for operational monthly forecasts). In this configuration, IFS is first integrated for ten days with a resolution of T399 (about 50 km resolution) and 62 vertical levels. At day 10 the horizontal resolution is lowered to T255 (about 80 km resolution) until the end of the forecast. During the first ten days, IFS is forced by persisted SST anomalies. After day 10, IFS is fully coupled to the HOPE (Hamburg Ocean Primitive Equation model) ocean GCM (Wolff et al. 1997). The frequency of coupling is 3 hours.

The initial conditions are taken from ERA40 (Uppala et al. 2005) until 2001 and from ECMWF operational analysis after 2001. The 14 perturbed integrations use slightly different atmospheric and oceanic initial conditions which are designed to represent the uncertainties inherent in the operational analyses. The 14 atmospheric perturbations are produced using the singular vector method (Buizza and Palmer 1995). These include perturbations in the Extratropics and perturbations in some tropical areas by targeting tropical cyclones (Puri et al. 2001). In addition, in order to take account of the effects of uncertainties in the model subgrid-scale parameterisations, the tendencies in the atmospheric physics are randomly perturbed during the model integrations(Buizza et al. 1999; Palmer 2001). Different ocean initial conditions are produced by applying a set of wind stress perturbations during the ocean data assimilation (Vialard et al. 2003). More details about the monthly forecast configuration at ECMWF can be found in Vitart et al. (2008).

3 Main characteristics of simulated MJO events

The methodology for assessing the skill to predict the MJO follows Gottschalck et al. (2009). The Wheeler and Hendon index (Wheeler and Hendon 2004) has been applied to all the model hindcasts and to ERA interim (Simmons et al. 2007) over the period 1989-2008 to evaluate the skill of the monthly forecasting system to predict MJO events and to produce composites for different phases of the MJO. The Wheeler and Hendon index is calculated by projecting the forecasts or analysis on the two dominant combined EOFs of outgoing longwave radiation (OLR), zonal wind at 200 and 850 hPa averaged between 15N and 15S. The index has been applied to daily anomalies relative to the 1989-2008 climate instead of the absolute value of the field, in order to remove the impact of seasonal cycle. In addition, a 120-day running mean has been subtracted to remove the variability associated to ENSO. The positive (negative) phase of EOF2 describes suppressed (enhanced) convection over the Indian ocean and enhanced (suppressed) convection over the West Pacific. The positive (negative) phase of EOF1 describes enhanced (suppressed) convection over the Maritime Continent region. Analysis and forecasts can be projected onto those two EOFs to describe the phase of the MJO in terms of two time series, PC1 and PC2. The two time series can be plotted as a succession of points in the PC1-PC2 phase space, in such a way that the MJO is described by a clockwise propagation in the phase space. The PC1-PC2 phase space can be divided into 8 sections representing a specific phase of the MJO (see for instance Figure 2 in Gottschalk et al. 2009). Phases 2 and 3 (negative EOF2) correspond to enhanced convection over the Indian ocean, phases 4 and 5 (positive EOF1) correspond to the MJO over the Maritime continent, phases 6 and 7 (positive EOF2) correspond to the MJO over the western Pacific and phases 8 and 1 (negative EOF1) correspond to the active phase of the MJO in the western Hemisphere.

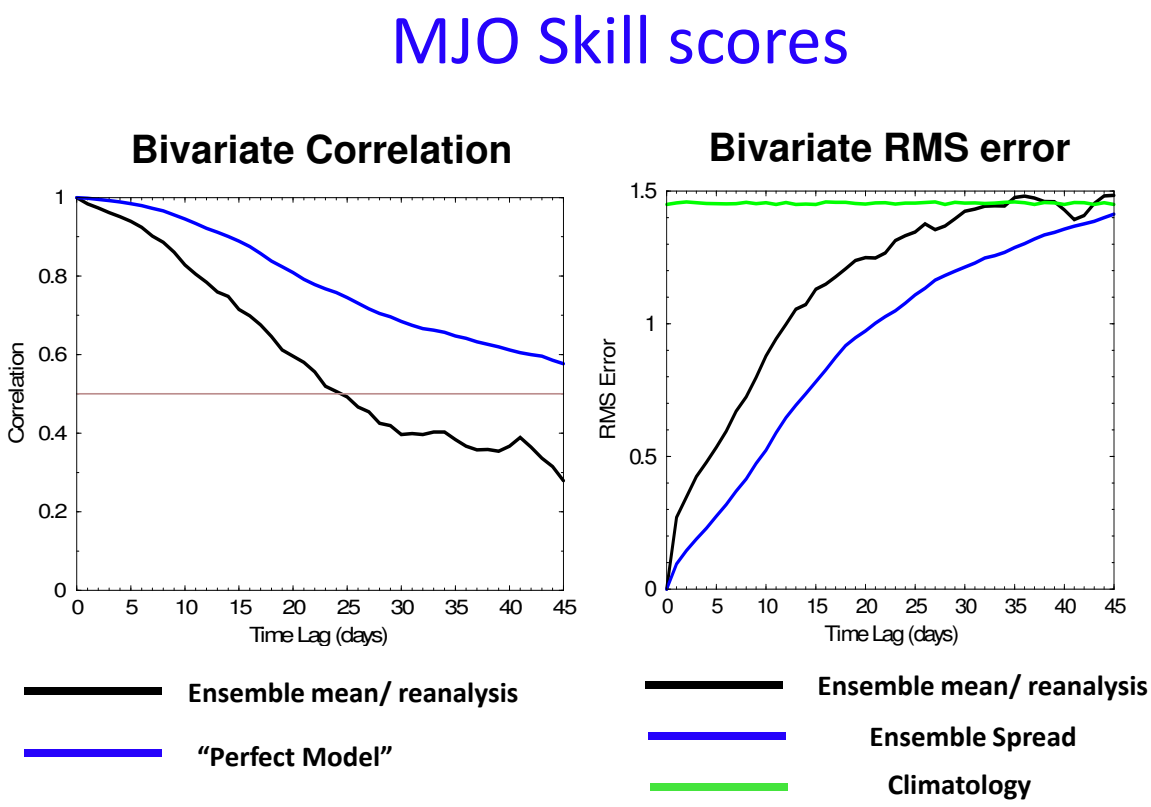

Figure 2: Bivariate correlation (left panel) and bivariate RMS error (right panel) between analysis and forecast PC1 and PC2 time series as a function of the forecast lead time for the period November to April 1989-2008 (black lines). The green line in the right panel shows the RMS error obtained with climatology. The blue line in the left panel shows the bivariate correlation obtained when considering one ensemble member to be the truth (perfect model assumption). In the right panel the blue line represents the ensemble spread.

Bivariate correlation and root mean square error are used to evaluate the skill of the dynamical model to predict the MJO as in Lin et al (2008) and Rashid et al. (2009). We consider that the forecast is skillful when the anomaly correlation is higher than 0.5.

According to Figure 2, the model ensemble mean has skill to predict the evolution of the MJO up to about day 23. PC1 and PC2 display similar correlations. The model potential predictability is evaluated using the ”perfect model” assumption: an ensemble member is considered to be the ”truth” and the ensemble mean is validated against this ensemble member. According to Figure 2, the model displays a potential predictability exceeding 45 days, which is far beyond the MJO predictability limit found by Waliser et al (2003). The bivariate RMS error of the ensemble mean the RMS error obtained with climatology after day 30. The ensemble spread is always smaller than the RMS error, which suggest that the ensemble spread is too small in this version of IFS. Those results indicate that model has useful skill up to day 20. The amplitude of the MJO simulated by the model starts increasing after day 5 and becomes too strong by about 20% after day 10 (not shown).

The monitoring of real-time forecasts from Cy32r3 indicates that the model often fails to propagate the

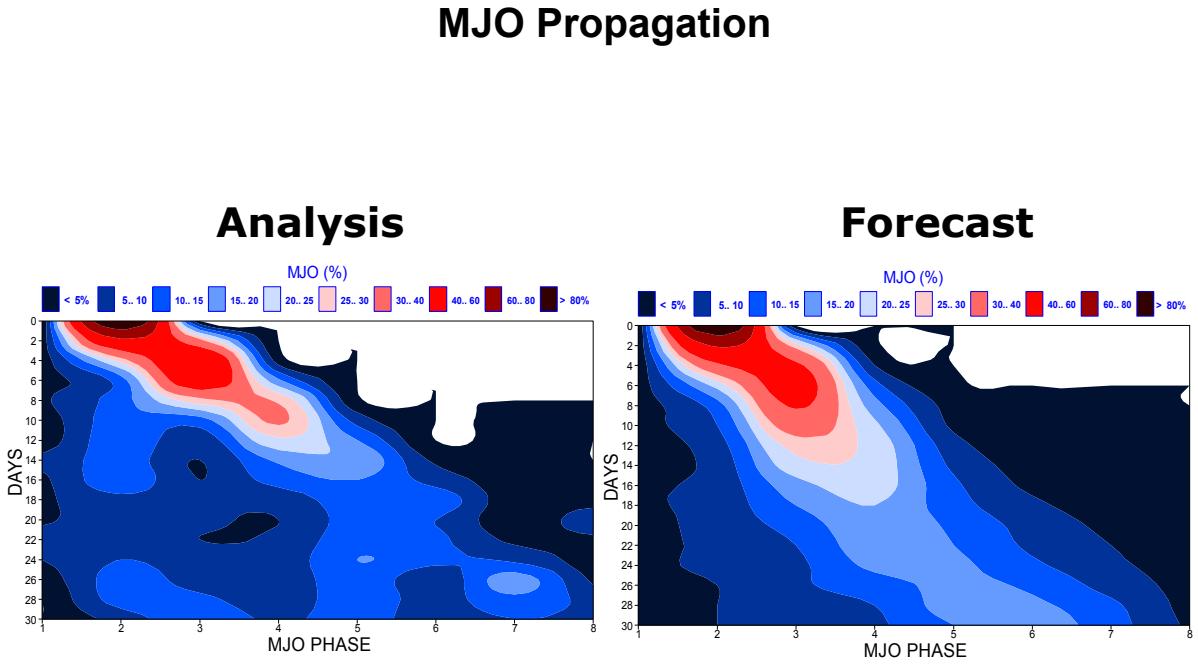

Figure 3: Hovmoeller diagram of the percentage of MJO events in a specific MJO phase as a function of lead time following an MJO in phase 2 (initial time). The left panel shows the eastward propagation in the reanalysis, and the right panel shows the eastward propagation of the MJO in the ensemble forecast.

MJO across the Maritime continent, and that it is often too slow over the Indian Ocean. To check if this is the case in the set of 46-day ensemble hindcasts, a composite of all the MJO events in phase 2 (convection over the western Indian Ocean) has been produced and its daily evolution calculated for the analysis and the ensemble hindcasts. A Hovmoeller diagram of the percentage of cases in a given phase of the MJO shows the eastward propagation of the MJO in both model and reanalysis, but the propagation is slower in the model than in the reanalysis (Fig. 3). For instance, the majority of MJO events in the reanalysis reach phase 4 within ten days after phase 2, instead of 14 days in the model simulations. All the 15 ensemble members display a too slow MJO propagation, suggesting that the difference in MJO speed between the model and reanalysis is statistically significant. This slow propagation of the MJO in the model is confirmed by the fact that the number of days spent on average in each individual phase of the MJO is higher in the model than in the reanalysis. It is not limited to the Indian Ocean, but also takes place over the Pacific and the western Hemisphere.

The percentage of events propagating from one phase of the MJO to the next phase is displayed in Table 1. The table shows that the percentage of events propagating over the Indian Ocean to the west of the

Maritime Continent (from phase 1 to 4) in the model hindcasts is close to the reanalysis. However, the percentage of MJO events crossing the Maritime continent (phase 4 to 5) and propagating into the west Pacific (phase 5 to 6) is lower in the model than in the reanalysis. In the reanalysis, 30% of MJO events do not propagate from the west part of the Maritime Continent into the western Pacific (from phase 4 to phase 6). This percentage climbs to 50% in the model. This confirms that the model has difficulties to propagate the MJO across the Maritime Continent. In addition, the model tends to regenerate too many MJOs from a previous MJO event: in the reanalysis, only 25% of MJOs in phase 7 start a new MJO event over the west Indian Ocean (phase 2). In the model, this percentage climbs to 40%.

	Phase $1 \mapsto 2$	Phase $2 \mapsto 3$	Phase $3 \mapsto 4$	Phase $4 \mapsto 5$	Phase $5 \mapsto 6$	Phase $6 \mapsto 7$	Phase $7 \mapsto 8$	Phase $8 \mapsto 1$
OBS	71%	81%	81%	80%	86%	79%	68%	55%
Model	71%	81%	80%	71%	72%	78%	65%	87%

Table 1: Percentage of MJO events moving from one MJO phase to another for observations (top row) and model hindcasts (bottom row).

4 Impact of the MJO on the northern Hemisphere weather

4.1 Impact on 500 hPa geopotential height anomalies

Using reanalysis data covering the period 1974-2007, Cassou (2008) showed that the impact of the MJO on European weather is the strongest about ten days after the MJO is in phase 3 or phase 6 (Figure 3 of Cassou 2008). The probability of a positive phase of the North Atlantic Oscillation (NAO) is significantly increased about ten days after the MJO is in phase 3 (phase 3 + 10 days), and significantly decreased about ten days after the MJO is in phase 6 (phase 6 + 10 days). The probability of a *negative* phase of the NAO is decreased (increased) about ten days after the MJO is in phase 3 (phase 6). The impact of the MJO on two other Euro-Atlantic weather regimes, the Atlantic Ridge and Scandinavian blocking, is much weaker. Lin et al (2010) also indicate that the MJO has an impact on the NAO and this impact is delayed by 2 to 3 pentads. This section will focus on phase 3 + 10 days and phase 6 + 10 days to evaluate if the model can reproduce the impact of the MJO on the NAO.

Figure 4 shows a 10-day lagged composite of 500 hPa geopotential height anomalies in the hindcasts and in ERA Interim for phases 3 and 6. The impact over the Euro-Atlantic sector is much weaker in the ensemble forecasts than in the 20 years of ERA Interim Reanalysis. For the 10-day lagged composite of

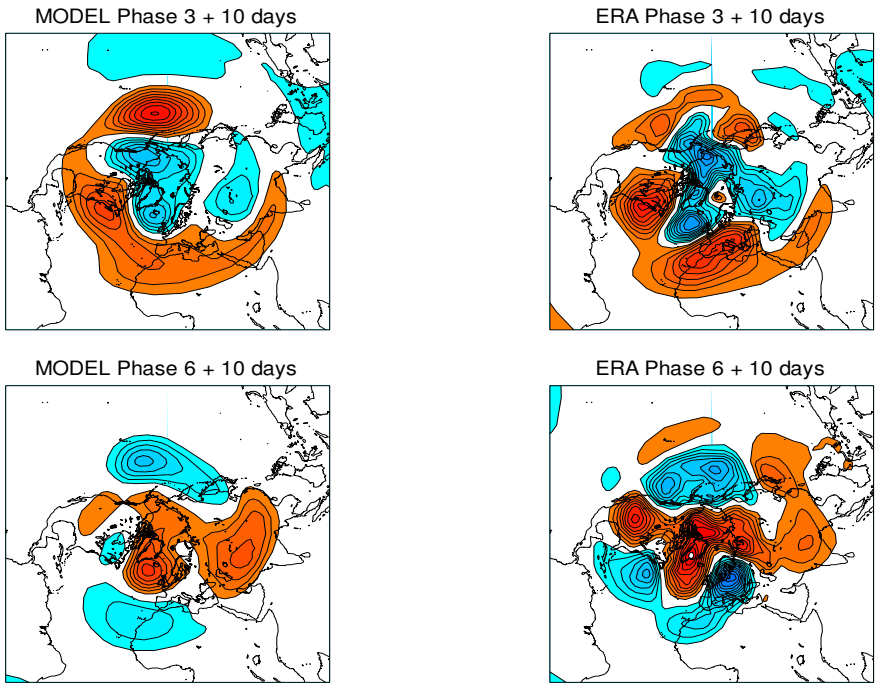

Figure 4: Phase 3 and 6 MJO 10-day lagged composites of 500 hPa geopotential height anomaly for the day 16-45 hindcasts (left panels) and ERA Interim (right panels). Red shadings indicate positive anomalies. Blue shadings indicate negative anomalies. The lowest contour is at 10 metres and the contour interval is 5 metres.

phase 3, the amplitude of the 500 hPa geopotential height anomalies is stronger in the model than in the reanalysis over the Pacific sector, but weaker over North-East Canada and Europe.

The fact that the MJO propagation in the model is too slow may have an impact on the MJO teleconnections. To test this hypothesis, the phase 3 + 10 days composites have been produced, but only for the MJO events simulated by the model which have a similar propagation speed as in the reanalysis (the criteria is that the MJO starting in phase 3 reaches phase 5 by day 8). Those composites were then compared to the MJO composites obtained from MJO events in the model which propagate slowly (the criteria is that the MJO is still in phase 3 by day 8). The lagged composites at day 10 indicate that the 500 hPa geopotential height anomalies over North East Canada and Europe are stronger with fast moving MJOs than with slow moving MJOs and are therefore more consistent with the reanalysis (Vitart and Molteni 2010). This result suggests that some of the discrepancies between the model simulations and ERA Interim could be due to the too slow MJO propagation in the model. However even the fast propagating MJO events simulated by the model fail to produce 500 hPa height anomalies over Europe as strong as in the reanalysis and the maximum of the positive anomaly is located too much to the South, over North Africa.

The impact of the MJO on the 500 hPa geopotential height anomalies depends also strongly on the intensity of an MJO event. Figure 5 shows that weaker MJOs (amplitude of the MJO index between 1 and 1.5 standard deviation) have significantly less impact over the northern Extratropics than strong MJOs (amplitude of the MJO index larger than 2 standard deviations). However since the model tends

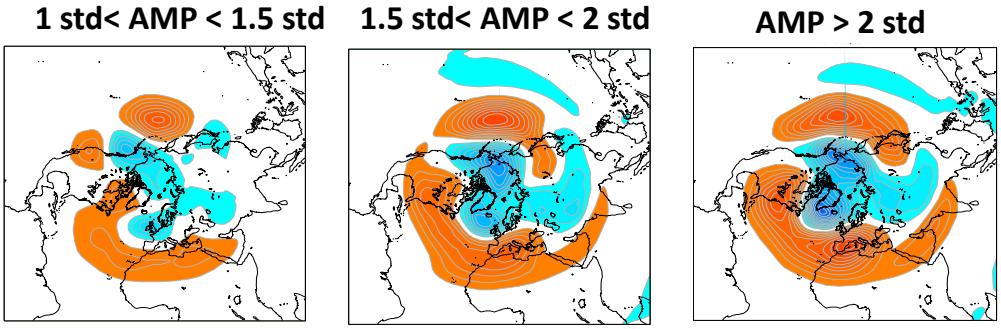

Figure 5: Phase 3 MJO 10-day lagged composites of 500 hPa geopotential height anomaly for the day 16-45 hindcasts when the amplitude of the MJO is between 1 and 1.5 standard deviations (left panel), between 1.5 and 2 standard deviations (middle panel) and more than 2 standard deviations (right panel). Red shadings indicate positive anomalies. Blue shadings indicate negative anomalies. The lowest contour is at 10 metres and the contour interval is 5 metres.

to produce stronger MJOs (see Section 3) this cannot explain the lower impact of the MJO over Europe in the model than in the reanalysis.

The same analysis was performed on a more recent version of IFS (Cycle 36r1 which was operational in the first half of 2010). According to Figure 6, the amplitude of the anomalies over Europe 10 days after an MJO in phase 3 is slightly larger than with Cycle 32r3, but the amplitude is still much smaller than in the reanalysis. To determine if this differences is due to the simulation of MJOs by the ECMWF forecasting system, a similar set of hindcasts was produced but this time the Tropics (between 20N and 20S) are relaxed towards reanalysis as in Jung et al. (2010). In this configuration, the model produces an MJO close to reanalysis. The relaxation experiment produces an MJO teleconnection which is more consistent with reanalysis. Interestingly the large 500 hPa height anomalies over North Pacific is strongly reduced in the relaxation experiment and is much more consistent with reanalysis than in the control experiment (experiment without relaxation). This suggests that the large discrepancy between model simulation and reanalysis over the North Pacific originates from the Tropics, possibly from systematic bias in the tropical Pacific. Over the Euro-Atlantic sector the amplitude of the teleconnections is also larger in the relaxation experiment than in the control experiment, but the amplitude of the anomalies is still significantly weaker in the relaxation experiment than in the reanalysis, by a factor 2 to 3. Therefore the difference in the amplitude of the MJO teleconnections over Europe cannot be explained by model errors in the Tropics.

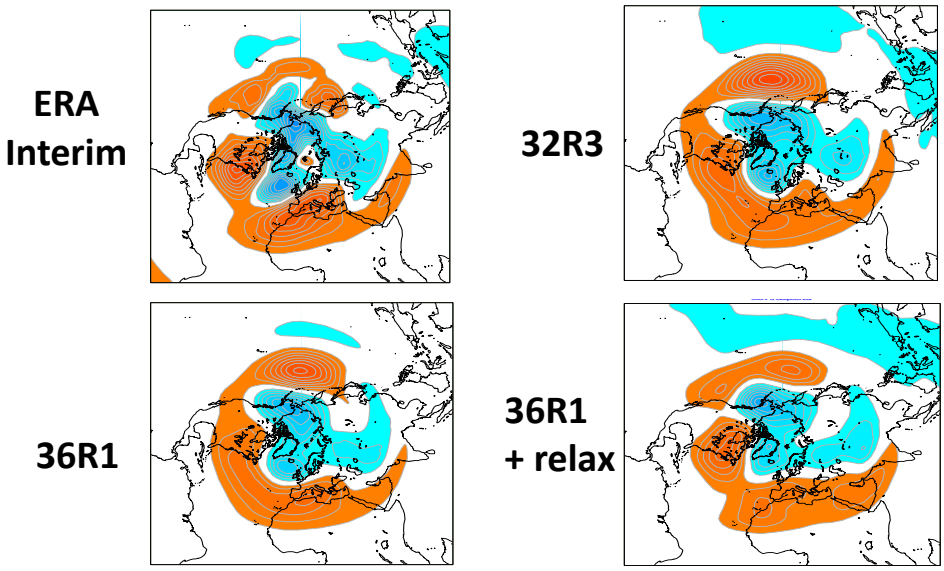

Figure 6: Phase 3 MJO 10-day lagged composites of 500 hPa geopotential height anomaly for the day 16-45 hindcasts in ERA Interim (top left panel), in the hindcasts performed with cycle 32R3 (top right panel), in the hindcasts performed with cycle 36r1 (bottom left panel) and in the hindcasts performed with cycle 36r1 and with the Tropics (20N-20S) relaxed towards reanalysis (bottom right panel).

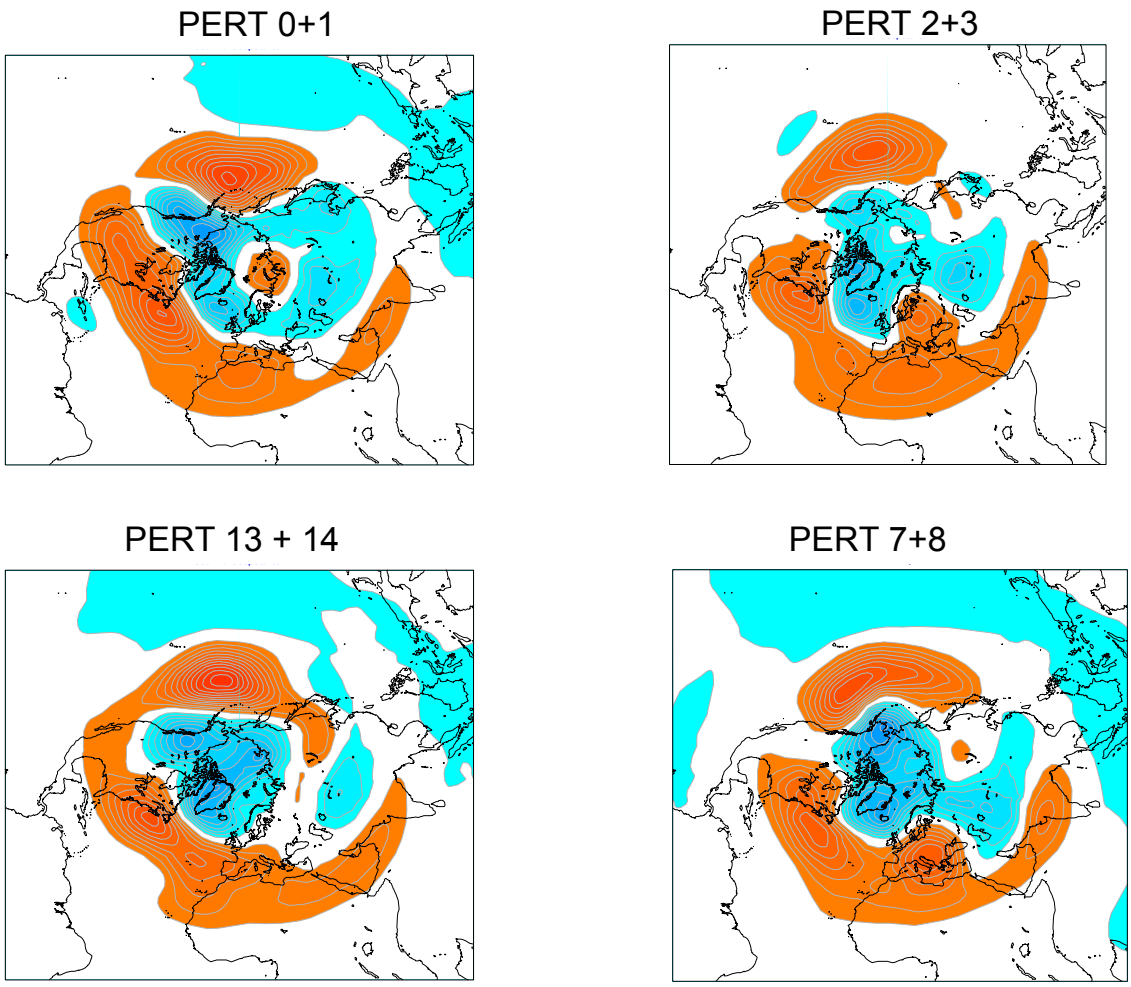

Figure 7: Same as Figure 4, but for ensemble members 0+1, 2+3, 13+14 and 7+8.

The model composites are produced over the equivalent of 300 years (15 member ensemble $\times$ 20 years) whereas the reanalysis dataset used in this study includes only 20 years. Therefore, it is possible that the strong signal over Europe in the reanalysis (Fig. 4) is due to sampling errors. To test if this is the case, the model composites have been computed for the combination of two individual ensemble members, instead of the combination of the 15 ensemble members. The combination of two ensemble members represents 40 years of forecast, which is twice the number of years in the reanalysis dataset used to produce the composites in Figure 4 and about the same number of years as the analysis dataset used by Cassou (2008). Figure 7 shows the phase 3 teleconnections after ten days for some combinations of two ensemble members. Some of the realisations (Pert 0+1 for instance) show a maximum positive anomaly over North Africa, when another one (Pert 2+3) shows a maximum over North-East Europe. Another realisation (Pert 13+14) has a maximum anomaly over the Atlantic, and another one (Pert 7+8) has a maximum anomaly over South-central Europe as in the 20-year ERA Interim reanalysis (Fig. 4). This suggests that there is considerable uncertainty in the impact of the MJO over the European sector, even in a 40 year simulation. The Pacific sector and western Canada display considerably less variability from one combination to another.

4.2 Impact on weather regimes

Another method to investigate the impact of the MJO on the Northern Extratropics weather is to project all the forecasts into pre-defined weather regime patterns. This is the method Cassou (2008) applied to an analysis covering the period 1974-2007. He found that the frequency of positive NAO regimes (NAO+) increases ten days after an MJO event in phase 3 and decreases ten days after an MJO event in phase 6. In the present paper, the model hindcasts and the ERA Interim reanalysis are projected onto 4 pre-defined weather regimes (NAO+, NAO-, Blocking, Atlantic ridge) for the period December-January-February 1989-2008. The pre-defined weather regimes have been computed by Corti and Ferranti (private communication) from ECMWF reanalysis data using the algorithm developed by Straus et al. (2002).

Figure 8 indicates that the probability of a NAO+ event increases with time during the 15 days following an MJO event in phase 3 in the majority of ensemble members. Only 3 ensemble members over 15 show a decrease of probability of NAO+ by day 15. This result suggests that the MJO simulated by the numerical model has an impact on the weather over Europe. The increased probability of a NAO+ event in the ensemble mean (about 20% at day 10) is only about half the increase obtained with ERA Interim (red line in Fig. 8). However the increase obtained with ERA Interim is within the spread of the 15-member ensemble, and there are a couple of ensemble members which show an increase of the probability of a positive NAO similar to the one obtained with ERA Interim. Therefore it is not clear if the discrepancy between the ensemble mean and ERA Interim is due to an inadequacy of the model to represent correctly the MJO teleconnections or if this is due to the fact that 20-year of reanalysis is too short to evaluate the impact of the MJO on weather regimes. The categorical definition of weather regimes may also contribute to the surprisingly large spread in Figure 8, since two relatively close weather patterns can be identified as different weather regimes. If we consider only the fast propagating MJO events (green curve in Fig. 8), the probability of NAO+ events increases slightly more than when considering all the MJO events, but the increase still remains lower than in ERA Interim.

The probability of a positive NAO diminishes during the days following an MJO event in phase 6 in both ensemble mean and ERA Interim (right panel of Fig. 8). The amplitude of the decrease of the probability of a positive NAO is of the same order of magnitude in the ensemble mean and in ERA Interim after day 10. The decrease obtained with ERA Interim is about half the amplitude of the increase obtained after an MJO in phase 3 and it is weaker than the decrease displayed in Figure 3 of Cassou (2008) where it reaches about 40%

Overall, the model displays a 10% decrease in the probability of a negative NAO (NAO-) in the 15 days period following an MJO event in phase 3 and a 12% increase in the 15 days period following an MJO event in phase 6 (Fig. 9). The sign of this variation of NAO- probability is consistent with ERA Interim and Cassou (2008), but the spread in the model ensemble distribution is particularly large. Only half of the ensemble members display a decrease of NAO- probability following an MJO in phase 3 or an increase following an MJO in phase 6. The amplitude of the changes in the probability of a negative NAO displayed by ERA Interim lies within the model ensemble distribution. As for the positive phase of the NAO, a few ensemble members show a similar evolution of the probability of a negative NAO as ERA Interim.

Nine ensemble members over fifteen (60%) simulate a steady decrease of the Scandinavian probability of a blocking following an MJO in phase 3 and an increase after phase 6. On average, the frequency of blockings is reduced by about 6% fifteen days after phase 3 and increases by about 10% ten days after phase 6 (Fig. 9).

The model simulates also an impact of the MJO on the probability of an Atlantic Ridge with an overall decrease after an MJO in phase 3 (66% of ensemble members) and an increase following an MJO in phase 6 (75% of ensemble members). Overall this represents a decrease or an increase of about 10% in

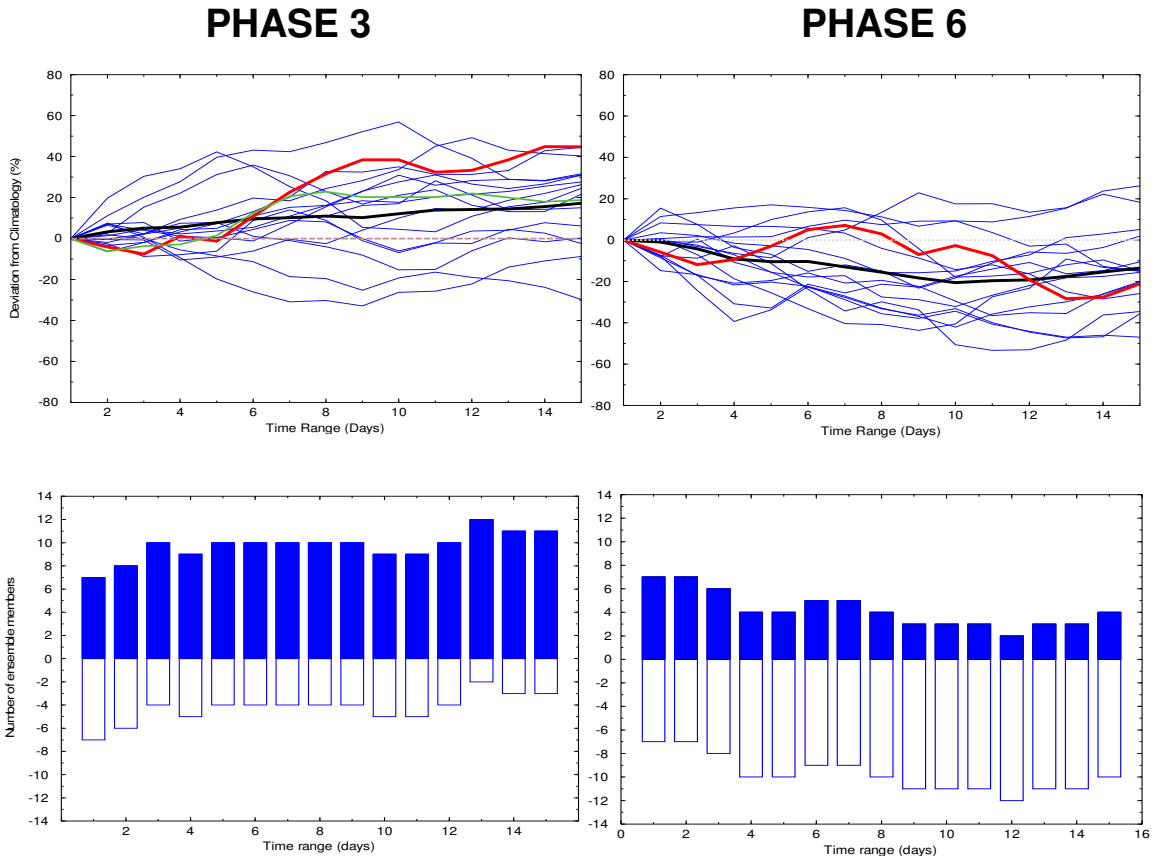

Figure 8: The top panels show the time evolution of the percentage of days in NAO+ relative to climatology as a function of lead time from phase 3 (left panel) and phase 6 (right panel). Each thin blue line represents an individual ensemble member. The solid black line represents the 15-member ensemble mean. The red line represents ERA Interim, and the green line in the top left panel represents the fast propagating MJO cases. The bottom panels show the number of ensemble members which display an increase (blue bars) or a decrease (white bars) of the frequency of NAO+ events.

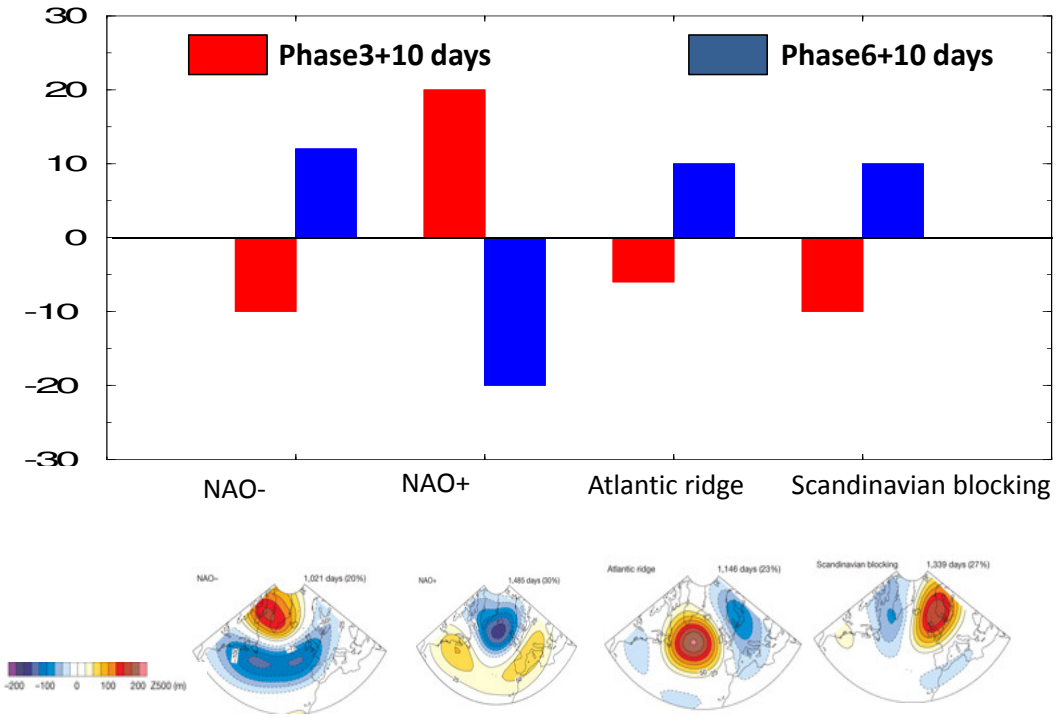

Figure 9: Variation of the percentage of days with NAO+, NAO-, Atlantic ridge or Scandinavian blocking 10 days after an MJO in Phase 3 (red bars) or Phase 6 (blue bars).

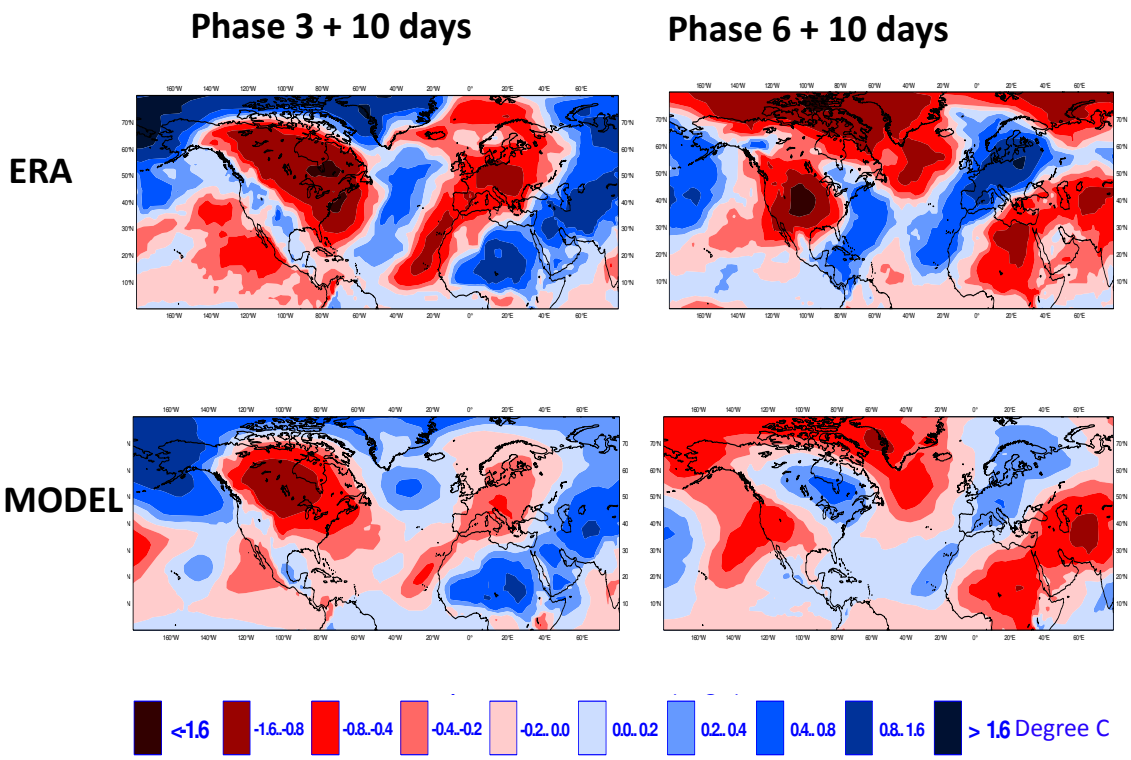

Figure 10: Composites of 2-metre temperature anomalies 10 days after an MJO in Phase 3 (left panels) and 10 days after an MJO in Phase 6 (right panels) in ERA Interim (top panels) and in the hindcasts (bottom panels).

the probability of an Atlantic Ridge by day 15 following an MJO respectively in phase 3 or 6 (Fig. 9).

As for NAO+ and NAO-, the impact of the MJO on the frequency of blockings and Atlantic Ridge is consistent with ERA Interim, although the amplitude is on average lower in the model simulations than in ERA Interim.

Since the MJO simulated by the model has an impact on the Euro-Atlantic weather regimes as in the reanalysis, the MJO simulated by the model is likely to impact the 2-metre temperature and precipitation anomalies over Europe. Figure 10 shows the anomalies of 2-metre temperature 10 days after an MJO in Phase 3 (left panels) and 10 days after an MJO in Phase 6 (right panels). In the days following an MJO in Phase 3 (Phase 6), the model tends to predict warmer (colder) 2-metre temperatures over Europe as in the reanalysis but with a weaker amplitude. Over North America and North Africa, the 2-metre temperature anomalies following an MJO in Phase 3 or 6 are generally consistent in the model and reanalysis, except over North America for Phase 6, where the cold anomaly simulated by the model is not at the same place as in the reanalysis (Fig. 10). The ECMWF forecast system simulates also an impact of the MJO on European precipitation consistent with reanalysis. Ten days after an MJO in Phase 3 (Phase 6), the model simulates wetter (dryer) conditions over North Europe and more (less) precipitation over southern Europe as in the reanalysis (not shown).

5 Impact of the MJO on the monthly forecast probabilistic skill scores

Previous studies (Ferranti et al. 1990; Jones et al. 2004; Jung and Palmer 2010) have suggested an improvement of forecast skill during MJO events. Ferranti et al. (1990) showed that a 20-day forecast was improved when the Tropics were relaxed towards observations during an MJO event. Jones et al. (2004) used a 10-year run of the NASA GCM to show that the potential predictability is increased by 2-3 days in that model. More recently, Jung and Palmer (2010) showed a reduction of extratropical forecast errors for periods with active MJO events in an experiment where the Tropics are relaxed towards observations as in Ferranti et al. (1990).

In the present paper, a different approach has been used to provide a more quantitative assessment of the impact of the MJO on the ECMWF monthly forecast probabilistic skill scores. The 120 15-member ensemble forecasts (all the forecasts starting on 15 October, November, December, January, February and March 1989-2008) have been classified as a function of the presence or not of an MJO event in the initial conditions. About 55% of the 120 cases have an MJO in the initial conditions (this MJO event can be in any phase). Probabilistic skill scores computed for all the cases with an MJO event in the initial conditions are then compared to the probabilistic skill scores computed for all the cases with no MJO event in the initial conditions. The probabilistic skill scores applied include the Relative Operating Characteristic (ROC) (Stanski et al. 1989; Mason and Graham 1999) and Brier skill scores (Wilks 2005) of the probability that 500 hPa geopotential height, 850 hPa temperature or total precipitation over the Northern Extratropics (North of 30N) are in the upper or lower tercile, for the weekly periods day 5-11, 12-18, 19-25 and 26-32. For precipitation and temperature only land points have been considered. The definition of the weekly periods (day 5-11, 12-18, 19-25 and 26-32) corresponds to the one used in the operational ECMWF monthly forecast products (Vitart 2004).

The Brier skill scores for the probabilities to be in the upper tercile are shown in Figure 11. The results for the low tercile probabilities (not shown) are similar. The results obtained with the ROC scores (not shown) are also similar. According to Figure 11, the Brier skill scores are not affected by the presence of an MJO in the initial conditions for the day 5-11 forecasts, except for precipitation with statistically significantly higher skill scores when there is an MJO in the initial conditions. For day 12-18, the Brier skill scores are significantly higher when there is an MJO in the initial conditions. For instance, the presence of an MJO in the initial conditions more than doubles the Brier skill score of 500 hPa geopotential height at this time range. The difference is statistically significant within the 10% level of confidence using a 10,000 bootstrap re-sampling procedure. The period day 19-25 is a time range often considered as having very low predictability and reliability in the Extratropics (see for example Vitart 2004 or Weigel et al. 2008). Therefore it is interesting to notice that when there is an MJO event in the initial conditions, the forecasts over the Northern Extratropics have a positive Brier Skill Score for 500 hPa geopotential height and temperature at 850 hPa for day 19-25, suggesting that those probabilistic forecasts are likely to be useful at this time range. When there is no MJO in the initial conditions, the day 19-25 forecasts have very low ROC area (close to 0.5) and negative Brier skill score, indicating that those forecasts have low skill and are not reliable. This result is confirmed by the reliability diagrams (Wilks 2005) (Fig. 12) of the probability that 850 hPa temperature is in the upper tercile for various regions, including Europe. Over Europe, the day 19-25 probabilistic forecasts display some reliability, with a reliability curve close to the diagonal, when there is an MJO in the initial conditions (red line in Fig. 12). However, the probabilistic forecasts are unreliable (almost flat curve) when there is no MJO in the initial conditions (blue line in Fig 12). This result suggests that the MJO represents a major, if not the main, source of predictability in the Northern Extratropics at this time range. This also demonstrates that the skill at this time range is not always as low as previous studies suggested and forecasts at this time range can be potentially useful over the northern Extratropics. From a practical point of view, this result also suggests that the users of the ECMWF monthly forecasting system could use the presence of an MJO in the initial conditions to decide if the monthly forecasts of day 19-25 should be trusted or not. For day 26-32, the presence of an MJO in the initial conditions also improves the probabilistic skill

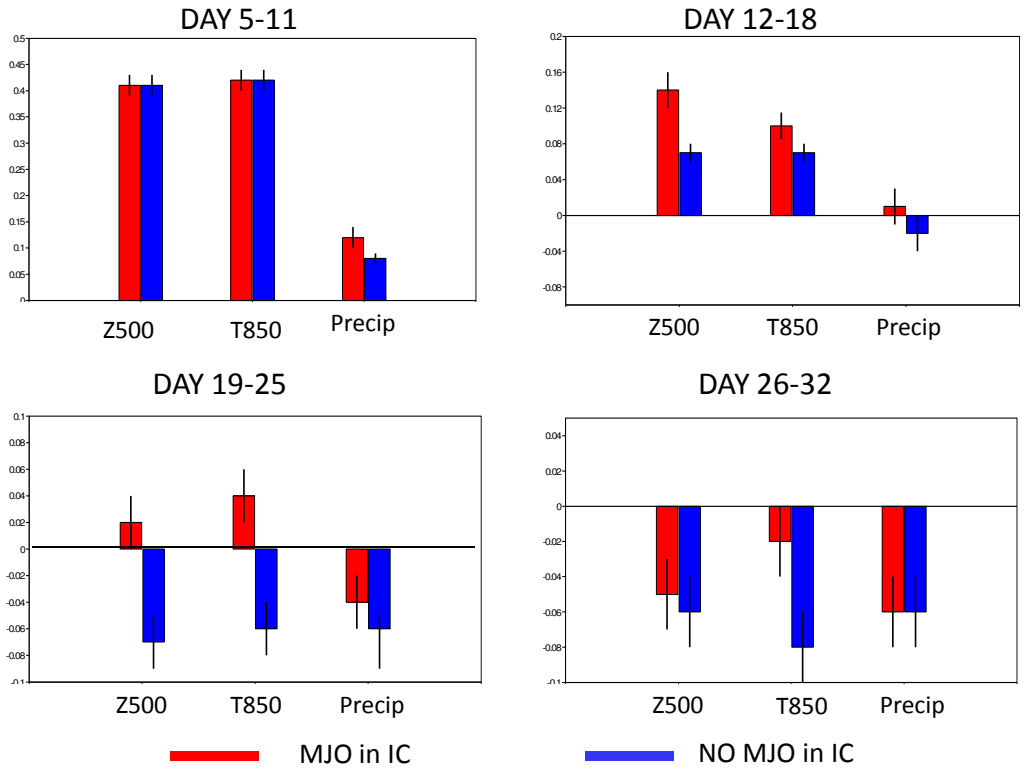

Figure 11: Brier skill scores of 500 hPa geopotential height, 850 hPa temperature and precipitation for day 5-11, 12-18, 19-25 and 26-32. The red bars show the scores obtained when there is an MJO in the initial conditions. The blue bars show the scores when there is no MJO in the initial conditions (amplitude of the MJO index less than 1 standard deviation). A 10,000 bootstrap re-sampling procedure has been applied to compute the 5% level of confidence (vertical black lines).

scores, but the probabilistic scores are very low, even with an MJO in the initial conditions.

Those results also suggest that improvements in the representation of the MJO in the ECMWF model are likely to lead to improved monthly forecast skill. Woolnough et al. (2007) have shown that coupling the atmospheric model to a high vertical resolution ocean mixed-layer model can impact the speed of the simulated MJO events through its impact on the SST diurnal cycle and intraseasonal variability. Therefore coupling IFS to an ocean mixed layer model, as in Woolnough et al. (2007), may help the atmospheric model to produce faster MJO events, which could lead to more realistic MJO teleconnections and enhanced skill in the Extratropics.

6 Impact of northern Extratropics on MJO skill scores

There has been evidence that the extratropics do have an influence on tropical convectively coupled waves in general (e.g. Kiladis and Weickmann 1992, Hoskins and Yang 2000) and the MJO in particular (e.g. Hsu et al. 1989, Lin et al. 2007, Wedi and Smolarkiewicz 2010, Ray and Zhang 2010). To

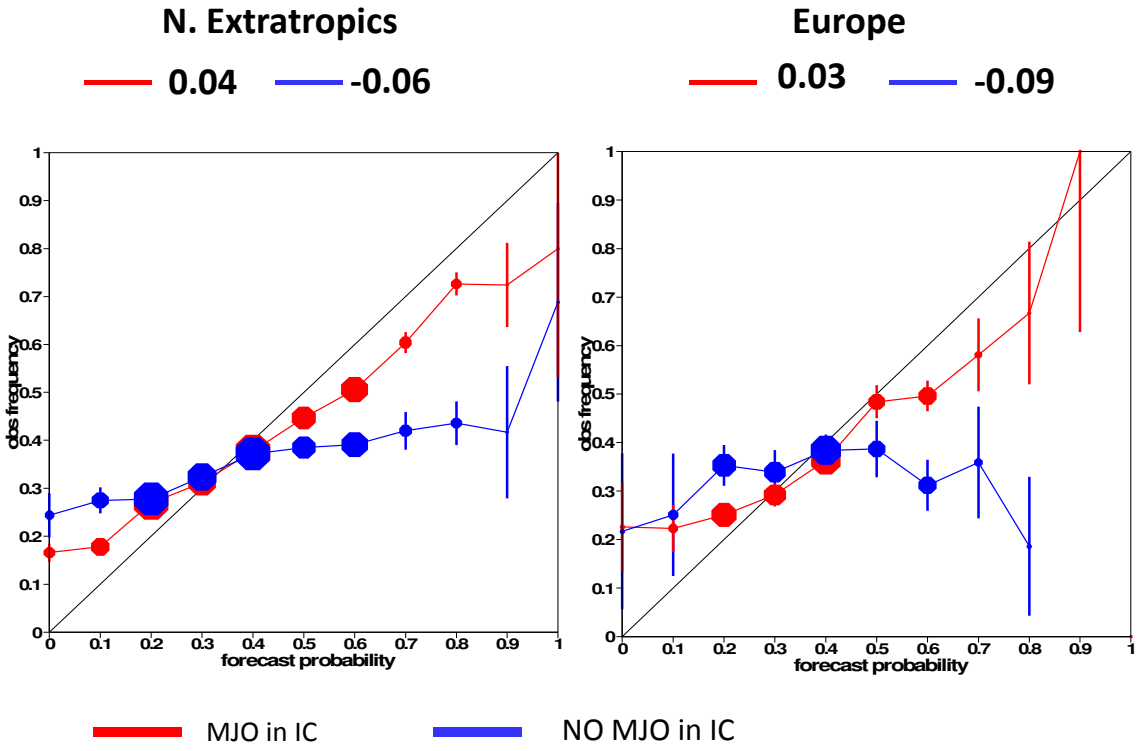

Figure 12: Reliability diagrams of the probability that the 850 hPa temperature is in the upper tercile for the period day 19-25 for the Northern Extratropics (left panel) and Europe (right panel). The red (blue) curves represent the reliability diagram obtained with all the cases with an MJO (no MJO) in the initial conditions. The volume of the symbols is proportional to the number of cases in the probability bin. A 10,000 bootstrap re-sampling procedure has been applied to compute the 5% level of confidence (vertical lines). The numbers on top of the figures indicate the Brier skill scores. Only land points have been included in the calculation of the reliability diagram and the Brier skill scores.

determine if this is the case in the ECMWF forecast system, a similar set of hindcasts as described in Section 3 has been performed but with the Northern Extratropics (defined here as North of 35N) relaxed towards reanalysis or initial conditions using the methodology described in Jung et al. (2010), and with a more recent version of IFS (cycle 36R1). In order to evaluate the impact of the northern Extratropics on the Madden Julian oscillation, the same hindcast experiments with and without relaxation have been carried out. The experiment without relaxation shall be called control integration (CNT hereafter). In the first relaxation experiment (REL-ANA), the northern Extratropics (North of 35N) are relaxed towards ERA Interim reanalysis data during the course of the integrations. In the second relaxation experiment (REL-INI), the northern Extratropics are relaxed towards initial conditions (i.e. persistence is enforced). The relaxation is carried out in grid point space for the zonal wind components, temperature and the logarithm of surface pressure. Further details of the method are described in Jung et al (2010a, 2010b). The comparison of the MJO forecast skill between REL-ANA and REL-INI will provide an estimate of the impact of the Northern Hemisphere extratropics on the MJO. The comparison between CTL and REL-ANA will provide an idea of how much more skill in predicting the MJO could be gained by improving forecasts of the northern Extratropics.

The bivariate correlation between the observations and the ensemble mean forecasts (i.e. the forecast skill) with the ECMWF monthly forecasting system is shown in Figure 12. The bivariate correlation falls to 0.6 at about day 26 (day 17) and to 0.5 by day 40 (day 22) in REL-ANA (REL-INI). These statistically significant results suggest that the northern Extratropics have a large impact on the skill of the model in predicting the MJO. The extratropical influence is larger for PC1 (propagation across the Maritime Continent and Africa) compared to PC2 (not shown). The impact of the northern Extratropics is statistically significant independently of whether there is a MJO present in the initial conditions or not (not shown). Generally, the extratropical influence is smaller when the MJO starts in Phase 6 or 7 (Convection over the Tropical Pacific) or in Phase 8 and 1 (MJO in the western Hemisphere) than when the convection associated with the MJO is located over the Indian Ocean (Phase 2 or 3) or over the maritime Continent (Phase 4 or 5) in the initial conditions. In order to identify which extratropical region has the largest influence on the MJO, the same series of hindcast was repeated but with the relaxation applied only on a part of the northern Extratropics. Results suggest that it is the western North Pacific (100E-180E, 35N-90N) which has the strongest impact on the MJO skill scores.

7 Conclusion

This paper has documented the main characteristics and impacts of the MJO in a set of 15-member ensemble hindcasts. The model displays some notable skill to predict the evolution of the MJO (about twenty days of predictability). However, the MJO simulated in this set of hindcasts suffers the following problems:

- The MJO simulated by the model tends to be too strong, but this has been partially solved in the following version of IFS.

- The simulated MJO tends to be too slow. This is not a systematic problem, since some MJOs in the model propagate at the same speed as observed MJOs, but on average the simulated MJO events tend to stay longer in each phase of the MJO.

- The simulated MJOs have often difficulties crossing the Maritime continent. Statistically the percentage of MJO events which do not cross the Maritime Continent is higher in the model than in observations. In those cases, the convection can be locked over the Maritime continent until the end of the 46-day forecast.

- The simulated MJOs tend to regenerate a new MJO too often.

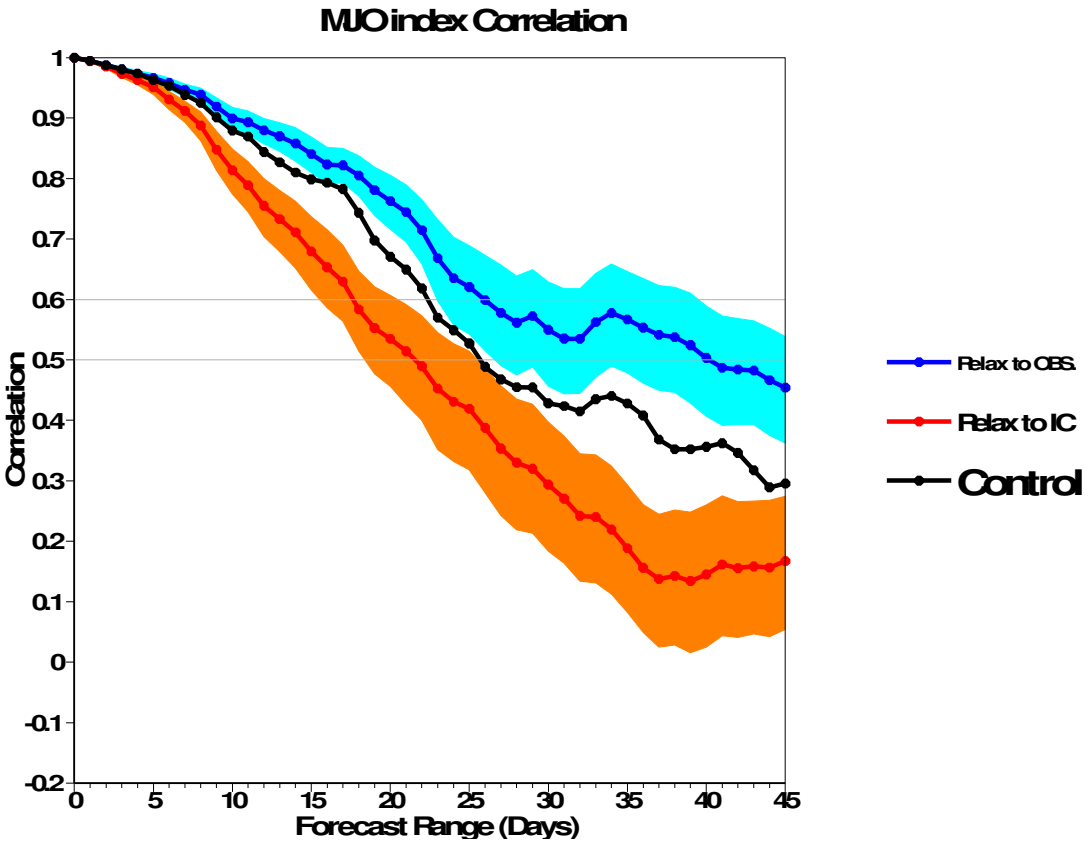

Figure 13: Bivariate correlation (forecast skill) as a function of the forecast lead time: control integration (CNT, black), relaxation of the Northern Hemisphere extratropical towards initial conditions (REL-INI, red) and analysis data (REL-ANA, blue) . The shaded areas represent 5% *level of confidence intervals computed using a bootstrap resampling technique.*

Of all those problems, the too slow propagation of the MJO is probably the most serious issue for the current ECMWF monthly forecasting system, particularly for the longer time range (day 19-25 and 26-32). The too slow propagation of the MJO and its difficulty to cross the Maritime Continent may cause the forecast to be out of phase with observations after twenty days in some occasions.

Vitart (2009) showed that the impact of the MJO on tropical cyclone activity and risk of landfall was also realistically simulated by the ECMWF model. In the Extratropics, the model simulates an increase in the probability of a positive NAO following an MJO in phase 3 (enhanced convection over the eastern Indian Ocean) and a decrease following an MJO in phase 6 (suppressed convection over the eastern Indian Ocean). Overall, the model teleconnections in the Extratropics are generally consistent with ERA Interim, except over the Euro-Atlantic sector where they are weaker than in ERA Interim. Fast propagating MJOs in the model display stronger teleconnections over Europe than slow propagating MJOs, but the teleconnections are still weaker than in ERA Interim. However the observed impact of the MJO on the Extratropics remains uncertain since twenty years of reanalysis may be too short to assess the MJO teleconnections in the mid-latitudes. The impact of the MJO on European 2-metre temperature and precipitation seems consistent with reanalysis, although the amplitude seems lower in the model than in the reanalysis.

The impact of the MJO on the extratropical forecast skill was investigated. Results show that the MJO has no significant impact for the period day 5-11, except for precipitation but has a a positive impact for day 12-18, 19-25 and 26-32. This impact is statistically significant for day 12-18 and 19-25. The impact of the MJO is particularly important for day 19-25 with the model showing almost no skill at all when there is no MJO in the initial conditions, but the day 19-25 probabilistic forecasts become reliable and skilful when there is an MJO in the initial conditions. This suggests that it is possible to know a-priori if a monthly forecast will be reliable or not. Those results also suggest that improvements in the representation of the MJO in the ECMWF model are likely to lead to improved monthly forecast skill.

A series of hindcast experiments has been performed in which the northern Extratropics are either relaxed towards reanalysis data (enforcing perfect extratropics) or initial conditions (enforcing persistence in the extratropics). In line with other recent studies (e.g. Wedi and Smolarkiewicz 2010 and Rau and Zhang 2010) these experiments suggest that the northern Extratropics do have a significant impact on the MJO and, therefore, on the skill of MJO forecasts. This impact originates mostly from the western North Pacific.

REFERENCES

Bechtold., P., M. Koehler, T. Jung, P. Doblas-Reyes, M. Leutbecher, M. Rodwell and F. Vitart, 2008: Advances in simulating atmospheric variability with the ECMWF model: From synoptic to decadal time scales, *Quart. J. R. Meteorol. Soc.*, **134**, 1337-1351.

Buizza, R. and T. N. Palmer, 1995: The singular-vector structure of the atmospheric general circulation. *J. Atmos. Sci.*, **52**, 1434-1456.

Buizza, R., M. Miller and T.N. Palmer, 1999: Stochastic representation of model uncertainties in the ECMWF Ensemble Prediction System. *Quart. J. Roy. Meteor. Soc.*, **125**, 2887-1908.

Cassou, C., 2008: Intraseasonal interaction between the Madden-Julian Oscillation and the North Atlantic Oscillation. *Nature*, doi:10.1038/nature07286.

Donald, A., H. Meinke, B. Power, A.H.N. Maia, M.C. Wheeler, N. White, R.C. Stone, and J. Ribbe, 2006: Near-global impact of the Madden-Julian oscillation on rainfall. *Geophy. Res. Lett.*, **33**, L09704, doi:10.1029/2005GL025155.

Ferranti, L., T. N. Palmer, F. Molteni and E. Klinker, 1990: Tropical-extratropical interaction associated with the 30-60 day oscillation and its impact on medium and extended range prediction. *J. Atm. Sci.*, **125**, 2177-2199.

Gottschalk J., M. Wheeler, K. Weickmann, F. Vitart, N. Savage, H. Hendon, H. Lin, M. Flatau, D. Waliser, K. Sperber, W. Higgins and A. Vintzileos, 2009: Establishing and Assessing Operational Model MJO Forecasts: A Project of the CLIVAR Madden-Julian Oscillation Working Group. *submitted to Bull. Am. Meteor. Soc.*

Hendon, H. H. and B. Liebmann, 1990: A composite study of onset of Australian summer monsoon. J. Atmos. Sci., **48**, 2909-2923.

Hoskins, B.J. and G.-Y. Yang, (2000), The equatorial response to higher-latitude forcing. *J. Atmos. Sci.*, **57**, 1197-1213.

Hsu, H.H., B.J. Hoskins, and F.-F. Jin (1990), The 1985/86 intraseasonal oscillation and the role of the extratropics, *J. Atmos. Sci.*, **47**, 823-839.

Jones, C., D. Waliser, K. Lau and W. Stern, 2004: The Madden-Julian Oscillation and its impact on Northern Hemisphere weather predictability. *Mon. Wea. Rev.*, **132**, 1462-1471.

Jung, T. and Palmer, T., 2010: Diagnosing the origin of extended-range forecast error. *Mon. Wea. Rev.*, **138**, 2434-2446.

Jung, T., T.N. Palmer, M.J. Rodwell, and S. Serrar 2010: Understanding the anomalously cold European winter of 2005/06 using relaxation experiments. *Mon. Wea. Rev.*,**138**, 3157-3174.

Kessler, K. S. and M. J. McPhaden, 1995: Oceanic equatorial Kelvin waves and the 1991-1993 El-Niño. *J. Climate*, **8** 1757-1774.

Kiladis, G.N., and K.M. Weickmann (1992), Circulation anomalies associated with tropical convection during northern winter. *Mon. Wea. Rev.*, **120**, 1900-1923.

Knutson, T. R. and Weickmann, K. M. 1987. 3060 day 51035113. atmospheric oscillations: Composite life cycles of convection and circulation anomalies.*Mon. Wea. Rev.*, **115**, 14071436.

Lin, H., G. Brunet, and J. Derome (2007), Intraseasonal variability in a dry atmospheric model. *J. Atmos Sci.*, **28**, 702-708.

Lin, H., G. Brunet, and J. Derome, 2008: Forecast skill of the Madden-Julian Oscillation in two Canadian atmospheric models. *Mon. Wea. Rev.*, 136, 4130-4149.

Lin, H., G. Brunet and J. Derome, 2009: An observed connection between the North Atlantic Oscillation and the Madden-Julian Oscillation. *J. Climate*, **22**, 364-380.

Lin. H., G. Brunet and R. Mo, 2010: Impact of the Madden-Julian Oscillation on wintertime precipitation over Canada. em Mon. Wea. Rev., in press.

Madden, R. A. and P.R. Julian, 1971: Detection of a 40-50 day oscillation in the zonal wind in the tropical Pacific. *J. Atm. Sci.*, **5**, 702-708.

Mason, S.J. and N.E. Graham, 1999: Conditional probabilities relative operating characteristics, and relative operating levels. *Wea. Forecasting*, **14**, 713-725.

Matthews, A.J., 2004: Intraseasonal variability over tropical Africa during northern summer. *J. Climate*, **17**, 2427-2440.

Matthews, A.J., B. J. Hoskins, and M. Masutani, 2004: The global response to tropical heating in the Madden-Julian Oscillation during Northern winter. *Quart. J. Roy. Meteor. Soc.*, **130**, 1991-2011.

Murakami, T., 1976: Cloudiness fluctuations during the summer monsoon, *J. Meteor. Soc. of Japan*, **54**, 175-181.

Nakazawa, T., 1986: Intraseasonal Variations of OLR in the tropics during the FGGE Year. *J. Met. Soc. Japan*, **64**, 17-34.

Palmer, T.N., 2001: A nonlinear dynamical perspective on model error: A proposal for nonlocal stochastic dynamic parameterisation in weather and climate prediction models. *Quart. J. Roy. Meteor. Soc.*, **127**, 279-304.

Puri, K., J. Barkmeijer, and T. N. Palmer, 2001: Tropical singular vectors computed with linearised diabatic physics. *Quart. J. Roy. Meteor. Soc.*, **127**, 709-737.

Rashid, H., H. H. Hendon, M. C. Wheeler, and O. Alves, 2009: Prediction of the Madden-Julian Oscillation with the POAMA dynamical prediction system. *Climate Dynamics*. DOI 10.1007/s00382-010-0754-x

Ray, P., and C. Zhang, (2010), A case study of the mechanics of extratropical influence in the initiation of the Madden-Julian Oscillation. *J. Atmos. Sci.*, **67**, 515-528.

Simmons, A., S. Uppala, D. P. Dee and S. Kobayashi, 2007: ERA-Interim: New ECMWF reanaly-

sis products from 1989 onwards, *ECMWF Newsletter*, **110**, 25-35.

Stanski, H.R., L.J. Wilson and W. R. Burrowa, 1989: Survey of common verification methods in meteorology. World Weather Watch Tech Rep. 8, WMO tech. DOC. 358, 114 pp.

Straus, D., S. Corti and F. Molteni, 2007: Circulation regimes: chaotic variability versus SST-forced predictability. J. Climate, 20, 2251-2272.

Uppala, S. M., and Coauthors, 2005: The ERA-40 re-analysis. *Quart. J. Roy. Meteor. Soc.*, **131**, 2961-3012.

Vialard, J., F. Vitart, M. A. Balmaseda, T. Stockdale and D. L. T. Anderson, 2003: An ensemble generation method for seasonal forecasting with an ocean-atmosphere coupled model. *Mon. Wea. Rev.*, **133**, 441-453.

Vitart, F, 2004: Monthly forecasting at ECMWF. Mon. Wea. Rev., **132**, 2761-2779.

Vitart, F., R. Buizza, M. A. Balmaseda, G. Balsamo, J.-R. Bidlot, A. Bonet, M. Fuentes, A. Hofstadler, F. Moleni and T. Palmer, 2008: The new VAREPS-monthly forecasting system: a first step towards seamless prediction. *Quart. J. Roy . Meteor. Soc.*, **134**, 1789-1799.

Vitart, F., 2009: Impact of the Madden Julian Oscillation on tropical storms and risk of landfall in the ECMWF forecast system. *Geophys. Res. Lett.*, L1 5802, doi:10.1029/2009GL039089.

Vitart, F. and F. Molteni, 2010: Simulation of the MJO and its teleconnections in the ECMWF forecast system. *Quart. J. Roy. Meteor. Soc.*, **136**, 842-855.

Waliser, D.E., W. Stern, and C. Jones: 2003: Potential predictability of the Madden Julian Oscillation. *Bull. Amer. Meteor. Soc.*, **84**, 33-50.

Wedi, N., and P.K. Smolarkiewicz, (2010), A Nonlinear Perspective on the Dynamics of the MJO: Idealized Large-Eddy Simulations. *J. Atmos. Sci.*, **67**, 1202-1217.

Weigel, A., D. Baggenstos, M.A. Liniger, F. Vitart and C. Appenzeller, 2008: Probabilistic verification of monthly temperature forecasts. *Mon. Wea. Rev.* , **136**, 5162-5182.

Wheeler, M.C. and H.H. Hendon, 2004: An all-season real-time multivariate MJO index: Development of an index for monitoring and prediction. *Mon. Wea. Rev.*, **132**, 1917-1932.

Wilks, D.S., 2005: *Statistical Methods in the Atmospheric Sciences. 2nd Edition*. Elsevier, 627 pp.

Wolff, J.O., E.Maier-Raimer, and S. Legutke, 1997: The Hamburg ocean primitive equation model. Deutsches Klimarechenzentrum Tech. Rep. 13, Hamburg, Germany, 98 pp.

Woolnough, S.J., F. Vitart and M. A. Balmaseda, 2007: The role of the ocean in the Madden-Julian Oscillation: Implications for MJO prediction. *Q. J. R. Meteorol. Soc.*, **133**, 117-128.